Very efficient boiling surfaces and their performance

Dong Ju Lee [a], Young Jae Yang[a], Dong Eok Kim [a*]
[a]*School of Energy System Engineering, Chung-Ang University, Seoul 06974, Korea*
**Corresponding author: dekim@cau.ac.kr*

1. Introduction

Boiling is a highly interested phenomenon in various nuclear engineering fields, such as core-to-coolant heat transfer in light water reactors (BWR & PWR), passive safety systems, and micro heat pipe reactor technology. In the boiling phenomenon, two key parameters are boiling heat transfer coefficient (BHTC) and critical heat flux (CHF). The BHTC and CHF determine boiling surface temperature and upper limit of heat transfer from surface to two-phase coolant, respectively. For the past decades, several methods had been developed to enhance the BHTC and CHF on a boiling surface, such as nanofluids [1,2], nano/micro porous structures [3-5], surface micromachining [6,7], chemical processes [8,9], and laser patterning [10,11]. In this paper, we introduce our progress to develop a boiling surface to highly enhance both BHTC and CHF using metal powder sintering process.

2. Methods

2.1 Experimental setup

Fig. 1(a) and (b) show the pool boiling setup and boiling substrate configuration, respectively. The pool boiling experiments were conducted under saturation condition ($T_{\text{sat}} = 100$ ℃) at atmospheric pressure using de-ionized water (DAEJUNG). The water was heated to the saturation temperature by single cartridge heater (1 kW) inserted in the boiling chamber. For removing non-condensable gas, the saturated water was heated for additional 30 min. before each experimental run. And, the temperature of working fluid was measured by two K-type thermocouples at two locations (top and bottom) in the chamber.

The boiling substrates were fabricated using silicon (Si) wafers (60×30 mm^2, thickness: 525 μm) with thermally deposited SiO_2 thin (thickness: 5,000 Å) layers on the top and bottom sides (see Fig. 1(b)). A platinum (Pt) thin film (30×10 mm^2, thickness: 1,200 Å) were deposited on the bottom side of Si-wafer by E-beam evaporation process. The Pt film was heated by Joule-heating method using a DC power supply (PSW 80V-40A, GWINSTEK). The electric current (I) and voltage drop(V) through the Pt film were measured using a current meter (MCR-S-10-50-UI-SW-DCI, Phoenix Contact) and voltage meter (MT4Y-DV-43, Autonics), respectively. The experimental data of temperatures, voltage, and current were acquired by using a data acquisition system (DAQ 970A, KEYSIGHT). The surface heat flux (q_s) was calculated as $q_s = \mathrm{VI}/A_s$, where A_s is the heating area of the Pt film. For measuring the boiling surface temperature, we used well-known temperature-electrical resistance linearity of Pt. Before each experimental run, The resistance of Pt heater was calibrated with actual temperature of that using constant temperature oven. The relation between the resistance and temperature of the Pt heater was obtained at four points ranged in 60-120 °C, and it showed very good linearity ($\mathrm{R}^2 > 0.9999$). For observing the boiling phenomena, a high-speed camera (Phantom M310) was utilized, and the boiling surface was illuminated with white-light LED (power: 120 W). The boiling images were obtained at the frame rate of 1,000 fps.

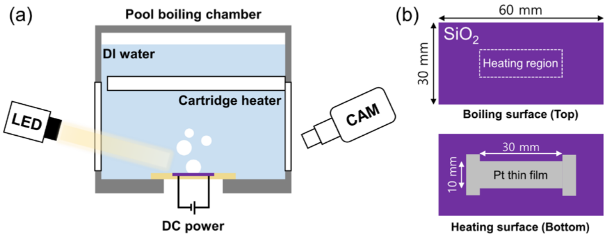

Fig. 1. (a) Pool boiling setup, (b) boiling substrate configuration.

2.2 Boiling surface preparation

Total four boiling surfaces were examined in this study. Table I shows the types of the boiling surfaces.

Table I: Types of the boiling surfaces.

Surface	Surface material and detail
Si-Bare	SiO_2, 5,000 Å thin film
Si-Cu	Cu, 2 μm thin film
Si-Cu-1L	Porous Cu layer, powder sintering
Si-Cu-Pil	Porous Cu layer+Cu pillars, powder sintering

For Si-Cu surface, Copper (Cu) thin film (thickness: 2 μm) was deposited on the Si-Bare surface by using RF sputtering process. For fabricating the Si-Cu-1L and Si-Cu-Pil surfaces, we utilized metal powder sintering technique. The Cu powders (99.9% Cu, spherical, Avention) were sintered on the Si-Cu surface using vacuum furnace under argon atmosphere (sintering temperature: 850 °C). Fig. 2 shows the Si-Cu, Si-Cu-1L, and Si-Cu-Pil surfaces.

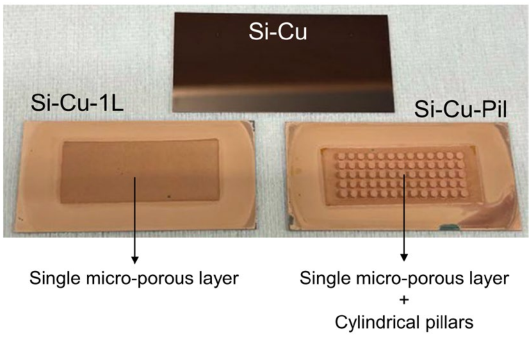

Fig. 2. Fabricated boiling surfaces.

In Si-Cu-Pil surface, each cylindrical pillar has dimensions of 2 mm diameter and 1 mm height. And, the center-to-center pitch of the pillars is 2.6 mm. Fig. 3(a) and (b) show the SEM picture of the micro porous structure on a boiling surface (Si-Cu-1L) and particle size distribution, respectively. As shown in the figure, the powder sintered boiling surface had several pores ranged from 1 μm to 10 μm scale, and the particle size was distributed mainly in the range of 10 to 50 μm.

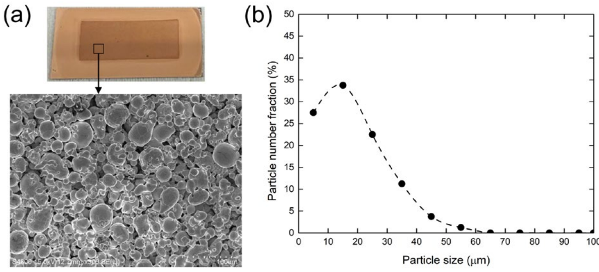

Fig. 3. (a) SEM picture of micro-porous boiling surface, (b) particle sized distribution of the boiling surface.

3. Results and discussion

Fig. 4 shows the pool boiling curves of four surface examined in this study. As shown in Fig. 4, the order of CHF values were Si-Bare < Si-Cu-1L < Si-Cu < Si-Cu-Pil. As a result, the CHF of Si-Cu-Pil surface was about 2.7 times higher than that of Si-Bare surface. Moreover, the wall superheat values of micro-porous structured surfaces, i.e., Si-Cu-1L and Si-Cu-Pil, were significantly lower than those of bare surfaces (Si-Bare and Si-Cu). This result indicates that the BHTC was highly enhanced by the role of micro-porous structures. Especially, Si-Cu-Pil substrate showed better boiling performance compared to the results of recent studies [12, 13] using metallic porous coatings (see Fig. 4). It might indicate the role of the porous pillar structures for inducing additional liquid supply by capillary wicking.

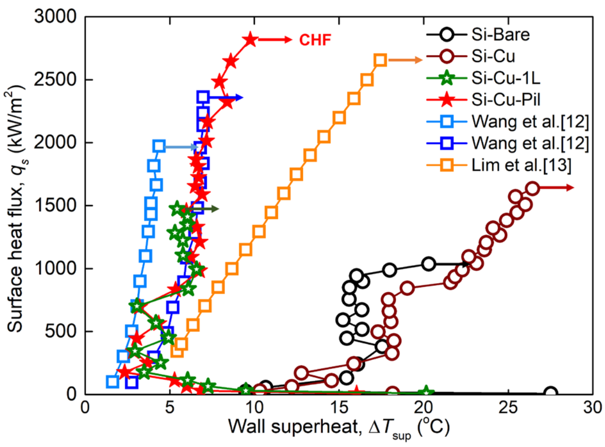

Fig. 4. Pool boiling curves.

As shown in Fig. 5, the bare surfaces (Si-Bare and Si-Cu) showed similar BHTC values, and also the surfaces with micro-porous structures (Si-Cu-1L, and Si-Cu-Pil) showed similar results. The maximum value of BHTC was recorded on Si-Cu-Pil surface with the value of 312.8 kW/m^{2}K which is about 5.3 times higher than that on Si-Bare surface. From the results of highly enhanced CHF and BHTC on Si-Cu-PiL, we guess that the micro-porous structures and millimeter size pillars affect the nucleate boiling behavior and liquid supply under high heat flux condition.

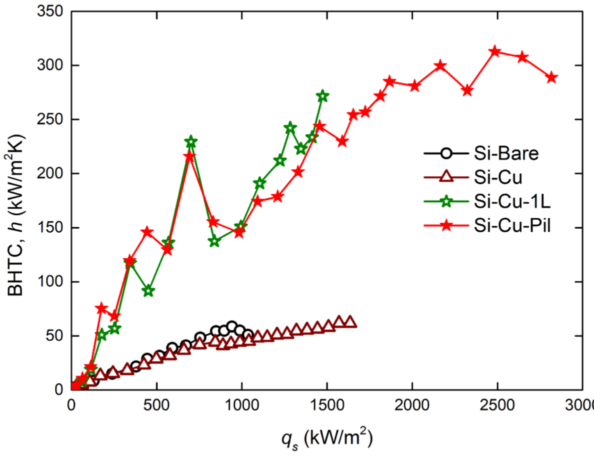

Fig. 5. Boiling heat transfer coefficient (BHTC) behaviors on four boiling surfaces.

Fig. 6 shows the vapor bubble behaviors of four boiling surfaces under low heat flux conditions. The bare and micro-porous surfaces show quite different behaviors. The nucleate site density of micro-porous surfaces is significantly higher than that of bare surfaces. And, very tiny bubbles are observed on the porous surfaces. The bubbles can highly enhance BHTC on the porous surfaces. We conjecture that the pores existed on the powder sintered surfaces act as nucleation cavities.

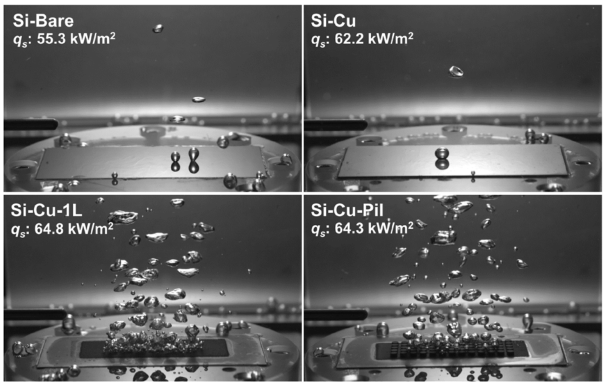

Fig. 6. Vapor bubble behaviors on different surfaces under low heat flux condition.

Fig. 7 shows the boiling behaviors on different surfaces under high heat flux conditions. On Si-Bare surface, a large vapor film is observed, and it indicates the boiling regime transition from nucleate boiling to film boiling. However, the nucleate boiling regime still maintains on other three surfaces. For Si-Cu surface, we guess that its surface wettability is better than that of Si-Bare surface. In the future work, we would measure the contact angle of sessile water drop on the surfaces. Next, for Si-Cu-Pil surface, we conjecture that the capillary wicking of liquids significantly enhance the rewetting of dry spots on the surface, i.e., the micro-structured pores in the porous pillar structures induce additional liquid flow into the boiling surface by capillary effect.

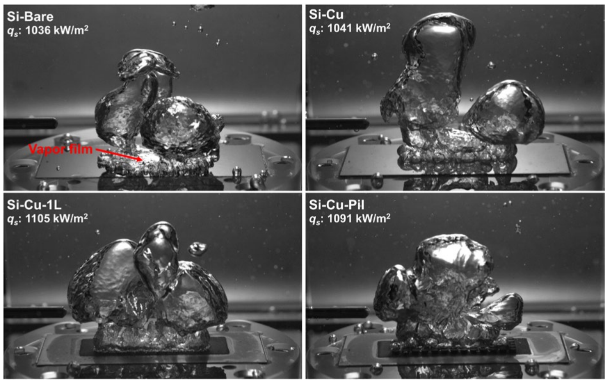

Fig. 7. Boiling behaviors on different surfaces under high heat flux condition

4. Conclusions

The results of this study are summarized as below:

- We fabricated various boiling surfaces to highly enhance the BHTC and CHF. The micro-porous surfaces could be fabricated by using metal powder sintering technique.
- The micro-porous structured boiling surfaces showed very high performance in the view of boiling BHTC and CHF.
- In the future work, we would try to reveal the original mechanism of the boiling performance enhancements on the micro-porous surfaces.

Acknowledgements

This study was supported by the National Research Foundation (NRF) grants funded by the Korean Government (Ministry of Science and ICT) (NRF-2022R1A2C1009970) and (RS-2023-00257279).

REFERENCES

[1] H.D. Kim, M.H. Kim, Effect of nanoparticle deposition on capillary wicking that influences the critical heat flux in nanofluids, Appl. Phys. Lett. Vol. 91, 014104, 2007.
[2] H. Kim, Enhancement of critical heat flux in nucleate boiling of nanofluids: a state-of-art review, Nanoscale Res. Lett. Vol. 6, pp. 415, 2011.
[3] S. Kim, H.D. Kim, H. Kim, H.S. Ahn, H. Jo, J. Kim, M.H. Kim, Effects of nano-fluid and surfaces with nano structure on the increase of CHF, Exp. Thermal Fluid Sci., Vol. 34, pp. 487-495, 2010.
[4] C.H. Li, T. Li, P. Hodgins, C.N. Hunter, A.A. Voevodin, J.G. Jones, G.P. Peterson, Comparison study of liquid replenishing impacts on critical heat flux and heat transfer coefficient of nucleate pool boiling on multiscale modulated porous structures, Int. J. Heat Mass Transfer, Vol. 54, pp. 3146-3155, 2011.
[5] D. E. Kim, D. I. Yu, Su Cheong Park, Ho Jae Kwak, H. S. Ahn, Critical heat flux triggering mechanism on micro-structured surfaces: Coalesced bubble departure frequency and liquid furnishing capability, Int. J. Heat Mass Transfer, Vol. 91, pp. 1237-1247, 2015.
[6]] R. Hosseini, A. Gholaminejad, M. Nabil, Concerning the effect of surface material on nucleate boiling heat transfer of R-113, J. Electron. Cooling Thermal Control, Vol. 1, pp. 22-27, 2011.
[7] S.G. Kandlikar, Controlling bubble motion over heated surface through evaporation momentum force to enhance pool boiling heat transfer, Appl. Phys. Lett., Vol. 102, 051611, 2013.
[8] Z. Yao, Y.W. Lu, S.G. Kandlikar, Effects of nanowire height on pool boiling performance of water on silicon chips, Int. J. Therm. Sci., Vol. 50, pp. 2084-2090, 2011.
[9] B.J. Zhang, K.J. Kim, H. Yoon, Enhanced heat transfer performance of alumina sponge-like nano-porous structures through surface wettability control in nucleate pool boiling, Int. J. Heat Mass Transfer, Vol. 55, pp. 7487-7498, 2012.
[10] J. Voglar, P. Gregorcic, M. Zupancic, I. Golobic, Boiling performance on surfaces with capillary-length-spaced one- and two-dimensional laser-textured patterns, Int. J. Heat Mass Transfer, Vol. 127, pp. 1188-1196, 2018.
[11] B. Liu, J. Liu, Y. Zhang, J. Wei, W. Wang, Experimental and theoretical study of pool boiling heat transfer and its CHF mechanism on femtosecond laser processed surfaces, Int. J. Heat Mass Transfer, Vol. 132, pp. 259-270, 2019.
[12] X. Wang, D. Fadda, J. Godinez, J. Lee, S.M. You, Effect of wettability on pool boiling heat transfer with copper microporous coated surface, Int. J. Heat Mass Transfer, Vol. 194, 123059, 2022.
[13] H. Lim, S-Y. Doh, J. Choi, J. Moc, S.M. You, J. Lee, Pool boiling heat transfer enhancement using the micro-thick metallic foam surface in saturated water, Int. Commun. Heat Mass Transfer, Vol. 152, 107310, 2024.